

**DEVELOPMENT OF ELECTROMECHANICAL PROPERTIES OF
BIOCOMPATIBLE GELATIN AS ACTUATOR APPLICATION**

Thawatchai Tungkavet

A Dissertation Submitted in Partial Fulfillment of the Requirements
for the Degree of Doctor of Philosophy
The Petroleum and Petrochemical College, Chulalongkorn University
in Academic Partnership with
The University of Michigan, The University of Oklahoma,
and Case Western Reserve University

2014

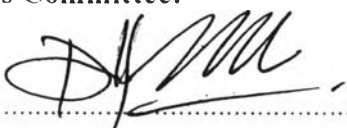
I 283708 18

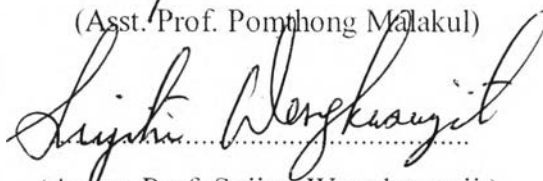
Thesis Title: Development of Electromechanical Properties of Biocompatible Gelatin as Actuator Application
By: Thawatchai Tungkavet
Program: Polymer Science
Thesis Advisors: Prof. Anuvat Sirivat
Dr. Nispa Seetapan

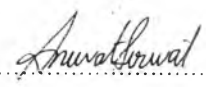
Accepted by The Petroleum and Petrochemical College, Chulalongkorn University, in partial fulfilment of the requirements for the Degree of Doctor of Philosophy.

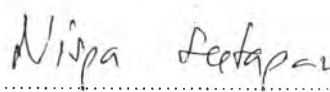

..... College Dean
(Asst. Prof. Pomthong Malakul)


Thesis Committee:


.....
(Asst. Prof. Pomthong Malakul)


.....
(Assoc. Prof. Sujitra Wongkasemjit)


.....
(Prof. Anuvat Sirivat)


.....
(Dr. Nispa Seetapan)


.....
(Dr. Datchanee Pattavarakorn)

ABSTRACT

5392004063: Polymer Science Program

Thawatchai Tungkavet: Development of Electromechanical
Properties of Biocompatible Gelatin as Actuator Application
Thesis Advisors: Prof. Anuvat Sirivat and Dr. Nispa Sectapan
164 pp.

Keywords: Actuator/ Biopolymer/ Gelatin/ Hydrogel/ Conducting polymers/
Stress relaxation

Nanowire-Polypyrrole/gelatin, MWNT/gelatin, and graphene/gelatin hydrogel composites were fabricated by the dispersion of nanofillers into the gelatin aqueous solution followed by the solvent casting. The electromechanical properties, thermal properties and deflection of pure gelatin hydrogel and nanowire-polypyrrole/gelatin, MWNT/gelatin, and graphene/gelatin hydrogel composites were studied as functions of temperature, frequency, and electric field strength as an actuator. The 0.01, 0.1, 0.5, 1 vol% these hydrogel composites and pure gelatin hydrogel possess a higher storage modulus sensitivity values ($\Delta G'/G'_0$) at a higher applied electric field strength in which graphene/gelatin hydrogel composites exhibit the greatest $\Delta G'/G'_0$, suggesting that it is the most suitable candidate for actuator applications. Nevertheless, the stress relaxation behavior as an important property for actuator. Uncrosslinked and crosslinked gelatin hydrogels were prepared by adding a glutaraldehyde solution into a gelatin solution followed by a casting method. Stress relaxation functions of the uncrosslinked and crosslinked gelatin hydrogels were measured to study the effects of electric field strength and the crosslinking ratio. For the uncrosslinked, 3 vol% crosslinked and 7 vol% crosslinked gelatin hydrogels, the relaxation times decrease with increasing degrees of crosslinking and the applied electric field strengths. The experimental shift factors can be thus obtained from either the stress relaxation functions or the storage and loss moduli. Both approaches yield numerically the same shift factor values which successfully allow the time-electric field superposition of various related functions.

บทคัดย่อ

รวิชัย ตุงคะเวทย์ : การพัฒนาคุณสมบัติการตอบสนองต่อสนามไฟฟ้าของเจลาตินเพื่อประยุกต์ใช้เป็นแอ็กชูเอเตอร์ (Development of Electromechanical Properties of Biocompatible Gelatin as Actuator Application) อ. ที่ปรึกษา : ศ.ดร. อนุวัฒน์ ศิริวัฒน์ และ ดร. นิสภา ศีตะปັນย์ 164 หน้า

วัสดุผสมเจลาตินไฮโดรเจลที่มีพอลิไพโรนุภากระดับนาโน อนุภาคคาร์บอนลักษณะแท่งผนังหลายชั้นระดับนาโน และกราฟีนผสมอยู่ถูกเตรียมด้วยการกระจายอนุภาคเหล่านี้ลงในสารละลายเจลาตินด้วยกรรมวิธีขึ้นรูปด้วยตัวทำละลาย คุณสมบัติเชิงกลทางไฟฟ้า คุณสมบัติทางความร้อน และคุณสมบัติการเปียงเบนของวัสดุภายในสนามไฟฟ้าของเจลาตินไฮโดรเจลบริสุทธิ์ เจลาตินไฮโดรเจลที่มีพอลิไพโรนุภากระดับนาโน เจลาตินไฮโดรเจลที่มีอนุภาคคาร์บอนลักษณะแท่งผนังหลายชั้นระดับนาโน เจลาตินไฮโดรเจลที่มีกราฟีนผสมอยู่ถูกศึกษาในความสัมพันธ์ของความร้อน ความถี่ และความแรงของสนามไฟฟ้าเพื่อประยุกต์เป็นแอ็กชูเอเตอร์ ปริมาณของสารเติมแต่งถูกผสมอยู่ในเจลาตินไฮโดรเจลด้วยอัตราร้อยละ 0.01, 0.1, 0.5, และ 1 โดยปริมาตรต่อปริมาตร และเจลาตินไฮโดรเจลบริสุทธิ์แสดงการตอบสนองความแข็งแรงของวัสดุที่เพิ่มขึ้นเมื่อให้ความแรงของสนามไฟฟ้าเพิ่มขึ้น ที่ซึ่งเจลาตินไฮโดรเจลที่มีกราฟีนผสมอยู่แสดงการตอบสนองความแข็งแรงของวัสดุได้สูงที่สุด นอกจากนี้พฤติกรรมการคลายตัวของความเค้นของวัสดุยังเป็นคุณสมบัติที่สำคัญสำหรับแอ็กชูเอเตอร์ด้วย เจลาตินไฮโดรเจลบริสุทธิ์ (ไม่ผ่านการเชื่อมขวางสายโซ่) และเจลาตินไฮโดรเจลที่ผ่านการเชื่อมขวางของสายโซ่ซึ่งเตรียมด้วยการเติมสารละลายกลูตาไรลดีไฮด์ (สารเชื่อมขวาง) ที่ความเข้มข้นต่าง ๆ ลงไปในสารละลายเจลาตินโดยกรรมวิธีขึ้นรูปแบบหล่อฟิล์ม การคลายความเค้นของเจลาตินไฮโดรเจลที่ไม่มีการเชื่อมขวางและเจลาตินไฮโดรเจลที่มีการเชื่อมขวางของสายโซ่ถูกศึกษาในอิทธิพลของความแรงของสนามไฟฟ้าและอัตราการเชื่อมขวางของสายโซ่ สำหรับเจลาตินไฮโดรเจลที่ไม่มีการเชื่อมขวางของสายโซ่ เจลาตินไฮโดรเจลที่มีการเชื่อมขวางของสายโซ่ที่ปริมาณสารเชื่อมขวางร้อยละ 3 และ 7 โดยปริมาตรต่อปริมาตร ตามลำดับ พบว่าเวลาที่ใช้ในการคลายความเค้นของวัสดุจะลดลงเมื่อเพิ่มอัตราการเชื่อมขวางของสายโซ่และความแรงของสนามไฟฟ้า ค่าชิฟเฟลคเตอร์ที่ได้จากการทดลองได้จากความสัมพันธ์ของการคลายความเครียดวัสดุ ความแข็งแรงวัสดุในเชิงของแข็ง ความแข็งแรงของวัสดุในเชิงของไหล ทั้ง 3 ความสัมพันธ์นี้ได้ค่าชิฟเฟลคเตอร์ออกมาในค่าเดียวกัน ซึ่งเป็นความสำเร็จสำหรับการศึกษา time-electric field superposition

ACKNOWLEDGEMENTS

The authors appreciate the financial supports provided by The Conductive and Electroactive Polymers Research Unit (CEAP) of Chulalongkorn University; The Thailand Research Fund (TRF); The Royal Thai Government; The 90th Anniversary of Chulalongkorn University Fund (Ratchadaphiseksomphot Endowment Fund); The Petroleum and Petrochemical College (PPC); The Center of Excellence on Petrochemical and Materials Technology; and The Doctoral Scholarship from The Thailand Graduate Institute of Science and Technology (TGIST) (TG-33-09-53-003D).

TABLE OF CONTENTS

	PAGE
Title Page	i
Abstract (in English)	iii
Abstract (in Thai)	iv
Acknowledgements	v
Table of Contents	vi
List of Tables	ix
List of Figures	xi
 CHAPTER	
I INTRODUCTION	1
 II THEORETICAL BACKGROUND AND LITERATURE SURVEY	 5
 III IMPROVEMENT OF ELECTROMECHANICAL PROPERTIES OF GELATIN HYDROGELS BY BLENDING WITH NANOWIRE-POLYPYRROLE: EFFECT OF ELECTRIC FIELD AND TEMPERATURE	 25
3.1 Abstract	25
3.2 Introduction	26
3.3 Experimental	27
3.4 Results and Discussion	31
3.5 Conclusions	37
3.6 Acknowledgements	38
3.7 References	39

CHAPTER	PAGE
IV STRESS RELAXATION BEHAVIOR OF (ALA-GLY-PRO-ARG-GLY-4HYP-GLY-PLO-) GELATIN HYDROGELS UNDER ELECTRIC FIELD: TIME-ELECTRIC FIELD SUPERPOSITION	54
4.1 Abstract	54
4.2 Introduction	55
4.3 Experimental	57
4.4 Results and Discussion	62
4.5 Conclusions	67
4.6 Acknowledgements	68
4.7 References	69
V ELECTROMECHANICAL PROPERTES OF MULTI-WALLED CARBON NANOTUBE/GELATIN HYDROGEL COMPOSITES: EFFECTS OF ASPECT RATIOS, ELECTRIC FIELD, AND TEMPERATURE	81
5.1 Abstract	81
5.2 Introduction	82
5.3 Experimental	83
5.4 Results and Discussion	86
5.5 Conclusions	94
5.6 Acknowledgements	94
5.7 References	95
VI INFLUENCE OF ELECTRIC FIELD, TEMPERATURE, AND SURFACE AREA ON ELECTROMECHANICAL PROPERTIES OF GRAPHENE/GELATIN HYDROGEL COMPOSITES	111
6.1 Abstract	111

CHAPTER	PAGE
6.2 Introduction	112
6.3 Experimental	113
6.4 Results and Discussion	117
6.5 Conclusions	124
6.6 Acknowledgements	125
6.7 References	125
VII CONCLUSIONS AND RECOMMENDATIONS	144
REFERENCES	147
CURRICULUM VITAE	162

LIST OF TABLES

TABLE		PAGE
CHAPTER II		
2.1	Comparative chart on the mechanical, thermal and electrical properties of graphene with CNT, steel, plastic, rubber, and fiber	16
CHAPTER III		
3.1	FTIR characteristic peaks of synthesized polypyrrole	52
3.2	Average particle sizes and electrical conductivity data of Ppy synthesized at different DBSA/pyrrole ratios	52
3.3	Sensitivity of the storage modulus of the pure gelatin and the Nanowire Ppy/gelatin hydrogels: 0.15 %strain, electric field strength 800 V/mm, frequency of 100 rad/s, and at 30 °C	53
CHAPTER IV		
4.1	Relaxation parameters of uncrosslinked, 3 %v/v crosslinked and 7 %v/v crosslinked gelatin hydrogels at various electric field strengths, at 25 °C and 0.20 %strain	79
4.2	Material constants (C_T) of uncrosslinked, 3 %v/v crosslinked and 7 %v/v crosslinked gelatin hydrogels at various reference electric field strengths (V/mm)	80
CHAPTER V		
5.1	Determination of density, diameter, and conductivity of Multi-walled Carbon Nanotubes (MWNTs)	109

TABLE	PAGE
5.2 Sensitivity of storage modulus of the pure gelatin hydrogel and the MWNT (2100)/gelatin hydrogels (0.10 %strain, electric field strength 800 V/mm, frequency 100 rad/s, 30 °C)	109
5.3 Induction time of MWNT/Gelatin hydrogel at various electric field strengths from deflection measurement: (a) pure gelatin hydrogel; (b) 0.1 vol% MWNT/Gelatin hydrogel; (c) 1 vol% MWNT/Gelatin hydrogel	110
CHAPTER VI	
6.1 Determination of density, diameter, surface area, and conductivity of graphene	141
6.2 Sensitivity of storage modulus of the pure gelatin hydrogel and the graphene/gelatin hydrogels (0.10 %strain, electric field strength 800 V/mm, frequency 100 rad/s, 30 °C)	142
6.3 Comparison of the storage modulus sensitivities ($\Delta G'/G'_0$) of electroactive and dielectric elastomer materials at temperature testing 27 °C	143

LIST OF FIGURES

FIGURE		PAGE
CHAPTER II		
2.1	Examples of conductive polymers (CPs): (a) Polyacetylene; (b) Polypyrrole; (c) Polythiophene; (d) Polyphenylene vinylene; (e) Polyaniline; (f) Poly(p-phenylene).	7
2.2	Electroactive responses under electric field.	8
2.3	Electronic band in neutral, polaron, bipolaron, and bipolaron band in conductive polymers.	10
2.4	Possible mechanism of actuation ion (yellow/purple :A ⁻) and solvent (red/blue/gray) insertion between chain.	11
2.5	Graphene (top left) is a honeycomb lattice of carbon atoms. Graphite (top right) can be viewed as a stack of graphene layers. Carbon nanotubes are rolled-up cylinders of graphene (bottom left). Fullerenes (C ₆₀) are molecules consisting of a wrapped graphene through the introduction of pentagons on the hexagonal lattice.	15
2.6	(a) Applied strain and (b) Stress relaxation function for a viscoelastic material.	20
CHAPTER III		
3.1	Scheme of the possible interaction of the gelatin and dodecylbenzene sulfonic acid (DBSA).	43
3.2	SEM micrographs of DBSA-doped synthesized polypyrroles at various DBSA concentrations with a magnification of: (a) 0.0175 mol ($N_{\text{DBSA}}:N_{\text{monomer}} = 0.01:1$); (b) 0.175 mol ($N_{\text{DBSA}}:N_{\text{monomer}} = 1:1$); (c) 1.750 mol ($N_{\text{DBSA}}:N_{\text{monomer}} = 10:1$).	43

FIGURE	PAGE
3.3 SEM micrographs of cross-sections of the pure gelatin and the nanowire Ppy/gelatin hydrogels; (a) cross-section of the pure gelatin; (b) cross-section of the 0.1 %v/v nanowire Ppy/gelatin; and (c) cross-section of the 1 %v/v nanowire Ppy/gelatin.	44
3.4 AFM micrographs of: (a) Nanowire Ppy 0.1 %v/v /gelatin hydrogel; (a') Schematic diagram of nanowire Ppy 0.1 %v/v orientation; (b) Nanowire Ppy 1 %v/v /gelatin hydrogel; (b') Schematic diagram of nanowire Ppy 1 %v/v orientation; and (c) Pure gelatin hydrogel.	45
3.5 Temporal responses of the storage modulus (G') of the pure gelatin hydrogel and the nanowire Ppy /gelatin hydrogels (sample diameter 30 mm, gel thickness 1.405 mm, 0.15 %strain, frequency of 100 rad/s, electric field strength 800 V/mm, and at 30 °C): (\circ) pure gelatin hydrogel; (\square) 0.1 % v/v nanowire Ppy; (Δ) 1 %v/v nanowire Ppy.	46
3.6 Effect of concentration of particles on the storage modulus response ($\Delta G'$) at various electric field strengths (sample diameter 30 mm, gel thickness 1.405 mm, 0.15 %strain, frequency of 100 rad/s, and at 30 °C): (\circ) Pure gelatin hydrogel; (\square) 0.1 %v/v nanowire Ppy; and (Δ) 1 %v/v nanowire Ppy.	47
3.7 Effect of concentration of particles on the storage modulus (G') and the storage modulus response ($\Delta G'$) at various temperatures (sample diameter 30 mm, gel thickness 1.405 mm, 0.15 %strain, electric field strength 800V/mm, frequency of 100 rad/s).	48

FIGURE	PAGE
3.8 Schematic of the apparatus used to observe the dielectrophoretics on the hydrogel samples.	49
3.9 Deflection of the hydrogels at $E = 0$ and 600 V/mm : (a) pure gelatin hydrogel; (b) 0.1 %v/v nanowire Ppy/gelatin hydrogel; and (c) 1 %v/v nanowire Ppy/gelatin hydrogel. Note: The polarity of the electrode on the left hand side is positive.	50
3.10 (a) Deflection distances of the gelatin hydrogel, the 0.1 %v/v nanowire Ppy/gelatin hydrogel, and the 1 %v/v nanowire Ppy/gelatin hydrogel at various electric field strengths and (b) Dielectrophoretic force calculated through the Linear Deflection theory.	51

CHAPTER IV

4.1 (a) Stress relaxations of uncrosslinked and 7 %v/v crosslinked gelatin hydrogels at 0 and 800 V/mm and (b) stress relaxation master curves of uncrosslinked and 7 %v/v crosslinked gelatin hydrogels at electric field strengths between 0 and 800 V/mm (sample diameter 25 mm , gel thickness 0.988 mm , $25 \text{ }^\circ\text{C}$, 0.20 %strain).	73
4.2 (a) Storage modulus of uncrosslinked and 7 %v/v crosslinked gelatin hydrogels at 0 and 800 V/mm and (b) storage modulus master curves of uncrosslinked and 7 %v/v crosslinked gelatin hydrogels at electric field strengths between 0 and 800 V/mm (sample diameter 25 mm , gel thickness 0.988 mm , $25 \text{ }^\circ\text{C}$, 0.20 %strain).	74

FIGURE	PAGE
4.3 (a) Loss modulus of uncrosslinked and 7 %v/v crosslinked gelatin hydrogels at 0 and 800 V/mm and (b) loss modulus master curves of uncrosslinked and 7 %v/v crosslinked gelatin hydrogels at electric field strength varied between 0 and 800 V/mm (sample diameter 25 mm, gel thickness 0.988 mm, 25 °C, 0.20 %strain).	75
4.4 The experimental and modified shift factors of uncrosslinked, 3 %v/v crosslinked and 7 %v/v crosslinked gelatin hydrogels vs. electric field at the reference electric field of 0 V/mm (sample diameter 25 mm, gel thickness 0.988 mm, 25 °C, 0.20 %strain).	76
4.5 Superimpositions of the relaxation time distribution functions $H(\tau)$ of the gelatin hydrogels at various electric field strengths: (a) uncrosslinked gelatin hydrogels; (b) 3 %v/v crosslinked gelatin hydrogels and; (c) 7 %v/v crosslinked gelatin hydrogels (0.20 %strain, 25 °C, samples = 5).	77
4.6 (a) Topology image of uncrosslinked gelatin hydrogel and (b) EFM image under 5V of voltage bias of uncrosslinked gelatin hydrogel at 300K.	78
CHAPTER V	
5.1 SEM micrograph of cross-sections of the pure gelatin and MWNT/gelatin hydrogels (magnification of 60K): (a) cross-sections of the pure gelatin; (b) cross-section of the 0.1 vol% MWNT/gelatin hydrogel; and (c) cross-section of the 1 vol% MWNT/gelatin hydrogel.	99

FIGURE	PAGE
5.2 (a) Topology image of pure gelatin hydrogel; (a') EFM image under 5 V of sample voltage bias of pure gelatin hydrogel; (b) Topology image of 0.1 vol% MWNT/gelatin hydrogel; (b') EFM image under 5 V of tip voltage bias of 0.1 vol% MWNT/gelatin hydrogel; (c) Topology image of 1 vol% MWNT/gelatin hydrogel; (c') EFM image under 5 V of tip voltage bias of 1 vol% MWNT/gelatin hydrogel.	100
5.3 Degree of charge generated on MWNT/gelatin hydrogel under 5 V of tip bias at whole region.	101
5.4 Temporal responses of the storage modulus (G') of the pure gelatin hydrogel and the MWNT/gelatin hydrogels (sample diameter 30 mm, gel thickness 1.540 mm, 0.10% strain, frequency of 100 rad/s, 800 V/mm, 30 °C): pure gelatin hydrogel (\circ); 0.1 vol% MWNT/gelatin hydrogel (\square); 1 vol% MWNT/gelatin hydrogel (Δ).	102
5.5 Effect of aspect ratios of MWNT on the storage modulus response ($\Delta G'$) and storage modulus sensitivity ($\Delta G'/G'_0$) at various electric field strengths (sample diameter 30 mm, gel thickness 1.640 mm, 0.10% strain, frequency of 100 rad/s, 30 °C).	103
5.6 Effect of concentration of MWNT (2100) on the storage modulus response ($\Delta G'$) at various electric field strengths (sample diameter 30mm, gel thickness 1.640 mm, 0.10% strain, frequency of 100 rad/s, 30 °C).	104
5.7 Effect of concentration of MWNT (2100) on the storage modulus (G') and storage modulus response ($\Delta G'$) at various temperature (sample diameter 30 mm, gel thickness 1.640 mm, 0.10% strain, frequency of 100 rad/s, 800 V/mm).	105

FIGURE	PAGE
5.8 Schematic diagram of the apparatus used to observe the dielectrophoretics force on the hydrogel samples.	106
5.9 Deflection of the gelatin hydrogels at $E = 0$ and 600 V/mm : (a) pure gelatin hydrogel; (b) $0.1 \text{ vol\% MWNT/gelatin}$ hydrogel; (c) $1 \text{ vol\% MWNT/gelatin}$ hydrogel. (Note that the polarity of the electrode on the right-hand side is positive.)	107
5.10 (a) Deflection distance of the pure gelatin hydrogel, the $0.1 \text{ vol\% MWNT/Gelatin}$ hydrogel, and the $1 \text{ vol\% MWNT/Gelatin}$ hydrogel at various electric field strengths. (b) Dielectrophoretic force calculated through linear deflection theory.	108

CHAPTER VI

6.1 Schematic diagram of the apparatus used to observe the dielectrophoresis force on the hydrogel samples.	130
6.2 TEM micrographs of (a) graphene (CG) at magnification of 10K ; (b) graphene (MG) at magnification of 0.5K ; and (c) graphene (HG) at magnification of 0.5K .	131
6.3 SEM micrographs of pure gelatin and graphene/gelatin composites at magnification of 10K : (a) pure gelatin; (b) $0.01 \text{ vol\% graphene/gelatin}$ composite; (c) $0.1 \text{ vol\% graphene/gelatin}$ composite; (d) $0.5 \text{ vol\% graphene/gelatin}$ composite; (e) $1 \text{ vol\% graphene/gelatin}$ composite.	132

FIGURE	PAGE
6.4 (a) Topology image of pure gelatin hydrogel; (a') EFM image under 5V of sample voltage bias of pure gelatin hydrogel; (b) Topology image of 0.1 vol% graphene/gelatin hydrogel; (b') EFM image under 5V of tip voltage bias of 0.1 vol% graphene/gelatin hydrogel; (c) Topology image of 1 vol% graphene/gelatin hydrogel; (c') EFM image under 5V of tip voltage bias of 1 vol% graphene/gelatin hydrogel.	133
6.5 Degree of charge generated on graphene/gelatin hydrogel composites under 5 V of tip bias at whole region.	134
6.6 Temporal responses of the storage modulus (G') of the pure gelatin hydrogel and the graphene/gelatin hydrogels (sample diameter 30 mm, gel thickness 1.520 mm, 0.10 %strain, frequency of 100 rad/s, 800 V/mm, 30°C): pure gelatin hydrogel (\circ); 0.1 vol% MG/gelatin hydrogel (\square); and 1 vol% MG/gelatin hydrogel (Δ).	135
6.7 Effect of surface area of graphene on the storage modulus response ($\Delta G'$) and storage modulus sensitivity ($\Delta G'/G'_0$) at various electric field strengths (sample diameter 30mm, gel thickness 1.520 mm, 0.10 %strain, frequency of 100 rad/s, 30 °C).	136
6.8 Effect of concentration of MG/gelatin hydrogel on the storage modulus response ($\Delta G'$) at various electric field strengths (sample diameter 30mm, gel thickness 1.520 mm, 0.10 %strain, frequency of 100 rad/s, 30 °C).	137
6.9 Effect of concentration of graphene on the storage modulus (G') and storage modulus response ($\Delta G'$) at various temperatures (sample diameter 30mm, gel thickness 1.520 mm, 0.10 %strain, frequency of 100 rad/s, 800 V/mm).	138

FIGURE	PAGE
6.10 Deflection of the gelatin hydrogels at $E = 0$ and 600 V/mm : (a) pure gelatin hydrogel; (b) 0.1 vol\% graphene/gelatin hydrogel; (c) 1 vol\% graphene/gelatin hydrogel. (Note that the polarity of the electrode on the right-hand side is positive and the other is neutral)	139
6.11 (a) Deflection distance of the pure gelatin hydrogel, the 0.1 vol\% graphene/gelatin hydrogel, and the 1 vol\% graphene/gelatin hydrogel at various electric field strengths. (b) Dielectrophoretic force calculated through linear deflection theory.	140